Stability of the tumor suppressor merlin depends on its ability to bind paxillin LD3 and associate with β1 integrin and actin at the plasma membrane

Maria Elisa Manetti[1], Sandra Geden[1], Marga Bott[1], Nicklaus Sparrow[1], Stephen Lambert[2] and Cristina Fernandez-Valle[1,*]

[1]Burnett School of Biomedical Science and [2]Department of Medical Education, College of Medicine, University of Central Florida, Health Science Campus, 6900 Lake Nona Boulevard, Orlando, FL 32827, USA

*Author for correspondence (cfv@ucf.edu)

Biology Open 1, 949–957
doi: 10.1242/bio.20122121
Received 30th May 2012
Accepted 27th June 2012

Summary

The *NF2* gene encodes a tumor suppressor protein known as merlin or schwannomin whose loss of function causes Neurofibromatosis Type 2 (NF2). NF2 is characterized by the development of benign tumors, predominantly schwannomas, in the peripheral nervous system. Merlin links plasma membrane receptors with the actin cytoskeleton and its targeting to the plasma membrane depends on direct binding to the paxillin scaffold protein. Exon 2 of *NF2*, an exon mutated in NF2 patients and deleted in a mouse model of NF2, encodes the merlin paxillin binding domain (PBD1). Here, we sought to determine the role of PBD1 in regulation of merlin stability and association with plasma membrane receptors and the actin cytoskeleton in Schwann cells. Using a fluorescence-based pulse-chase technique, we measured the half-life of Halo-tagged merlin variants carrying PBD1, exon 2, and exons 2 and 3 deletions in transiently transfected Schwann cells. We found that PBD1 alone was necessary and sufficient to increase merlin's half-life from approximately three to eleven hours. Merlin lacking PBD1 did not form a complex with surface β1 integrins or associate with the actin cytoskeleton. In addition, direct binding studies using purified merlin and paxillin domains revealed that merlin directly binds paxillin LD3 (leucine-aspartate 3) domain as well as the LD4 and LD5 domains. Together these results demonstrate that a direct interaction between merlin PBD1 and the paxillin LD3–5 domains targets merlin to the plasma membrane where it is stabilized by its association with surface β1 integrins and cortical actin.

Key words: NF2, Merlin, Schwann cells, Paxillin, LD domain, β1 integrin, Actin

Introduction

The *NF2* gene encodes a 595 amino acid tumor suppressor named merlin and schwannomin (Rouleau et al., 1993; Trofatter et al., 1993). Loss of function of merlin is associated with Neurofibromatosis 2 (NF2), a disorder characterized by formation of multiple benign tumors in the nervous system. The predominant tumor types are schwannomas and meningiomas, but ependymomas, gliomas, and juvenile cataracts also occur. Ninety percent of the identified *NF2* mutations are frameshift, nonsense, and splice alterations predicted to generate truncated merlin proteins. The remaining 10 percent of mapped mutations are nucleotide substitutions primarily clustered in exons 2 and 3 that allow translation of a full-length, but mutant, protein. In frame deletions of exon 2 and exons 2 and 3 have also been documented in NF2 patients (Deguen et al., 1998; Ahronowitz et al., 2007). The high frequency of exon 2 mutations in the *NF2* gene indicates the functional importance of this coding region and prompted the development of a mouse model for NF2 in which exon 2 was conditionally deleted (Giovannini et al., 2000). Work form this laboratory previously identified a 21 amino acid paxillin binding domain encoded by exon 2 that is essential for the plasma membrane localization of merlin (Fernandez-Valle et al., 2002). In this study, we sought to determine if PBD1 is the only functionally important sequence encoded by exons 2 and 3, and to investigate how PBD1 promotes association of merlin with the plasma membrane.

Merlin shares sequence similarity with ezrin, radixin, and moesin (ERM) proteins, which belong to the Band 4.1 superfamily of cytoskeleton-associated proteins that link cell surface proteins to F-actin. Merlin/ERM proteins are made up of three structural domains: the amino (N)-terminal FERM domain that is subdivided into three subdomains (F1, F2, and F3), the α-helix domain, and the carboxy (C)-terminal domain, which contains a consensus direct binding site for actin in ERMs that is absent in merlin. The cytoskeletal activity of ERM proteins is regulated by conformational changes involving the association of the N- and C-terminal regions. The closed conformation is dormant and the open conformation is active because it exposes the actin binding domain and a number of binding sites within the FERM domain to peripheral and integral membrane proteins (Bretscher et al., 2002). Merlin undergoes similar conformational

changes and localizes to various subcellular compartments, including the plasma membrane, cytosol, and nucleus. Merlin's unique tumor suppressor activity was believed to be associated with action of the closed conformation in the cytosol (Gutmann et al., 1999; Morrison et al., 2001). However, more recently, merlin has been shown to influence trafficking and retention of mitogenic and adhesion receptors on the cell surface and to influence degradation of nuclear proteins (Maitra et al., 2006; Lallemand et al., 2009a; Li et al., 2010). These diverse functions have created confusion about merlin's mechanism of tumor suppression.

We believe that localization of merlin to the plasma membrane is an essential first step in density-dependent regulation of cell proliferation. Thus, we have focused on understanding the targeting and stabilization of merlin at the plasma membrane. Similar to ERM proteins, the open conformation facilitates localization of merlin to the membrane where it associates with receptors, and indirectly, with actin through a direct association with beta II-spectrin (Scoles et al., 1998; Grönholm et al., 1999). The open conformation is believed to be stabilized by phosphorylation of serine-518 by P21-activated kinase PAK (PAK) and cAMP-dependent protein kinase A (PKA) (Kissil et al., 2002; Xiao et al., 2002; Alfthan et al., 2004). Serine-518 phosphorylation is triggered by activation of β1 integrin and ErbB2/3 receptors in subconfluent Schwann cells (SCs) (Thaxton et al., 2008) and these receptors are essential for SC motility on axons, proliferation, and myelination (Chernousov et al., 2008).

We previously demonstrated a direct association between merlin and paxillin (Fernandez-Valle et al., 2002). Specifically, we mapped two direct paxillin binding domains, one of which, PBD1, spans residues 50–70, is encoded by exon 2, and is absolutely required for translocation of merlin to the plasma membrane and its phosphorylation at serine-518 (Fernandez-Valle et al., 2002; Thaxton et al., 2008). Paxillin is a multi-domain adaptor protein that recruits receptor tyrosine kinases to focal adhesions, integrates signals from the extracellular matrix (ECM), and regulates actin organization (Turner, 2000; Schaller, 2001). Within the N-terminus there are five LD protein recognition motifs (Brown et al., 1998). LD1, 2, and 4 directly bind vinculin, focal adhesion kinase (FAK), PAK, guanine nucleotide exchange factor (PIX), and additional proteins (Turner et al., 1990; Turner et al., 1999) involved in focal adhesion formation and signaling. No binding partner has been identified for LD3. The C-terminus of paxillin contains four LIM (Lin11, lsl-1, Mec-3) domains that mediate protein-protein interactions and are essential for paxillin targeting to focal adhesions (Turner, 2000).

In the present study, we explored the functional role of PBD1 in controlling the stability of merlin and its interactions at the plasma membrane. We report that the 21 amino acid PBD1 is the domain in *NF2* exons 2 and 3 that is actively involved in controlling the half-life of merlin and its interaction with β1 integrin and actin at the plasma membrane. Moreover, we identified paxillin LDs 3, 4, and 5 in merlin as direct binding sites.

Results

Sequence alignment of PBD1 of various species

We traced the evolutionary origin of PBD1 using sequence-based analysis. First, we analyzed the sequence similarity of merlin in various vertebrate species, including humans (*Homo sapiens*), primates (*Papio anubis*), rats (*Rattus norvegicus*), chicken (*Gallus gallus*), and zebrafish (*Danio rerio*), by performing pairwise alignment of the entire merlin sequence using ClustalW2. We found that merlin was conserved in mammals, with an identity higher than 95%. By contrast, when we compared mammals and evolutionarily distant species, such as *Caenorhabditis elegans* and *Drosophila melanogaster*, the amino acid identity was less than 50%. PBD1 was the only sequence in the FERM F1 domain encoded by human exons 1 and 2 that was conserved across all species. PDB1 has a contiguous stretch of 13 amino acids that have identical (*) or conserved (:) substitutions (Fig. 1A). Previous phylogenetic analysis of the FERM domain showed that ERM proteins and merlin form an orthologous group (Bretscher et al., 2002). Based on this information, we included human ERM sequences in the alignment analysis and found that PBD1 remained a recognizably conserved domain (supplementary material Fig. S1). However, when we compared human protein 4.1 and talin (GeneBank No: AAD42222 and

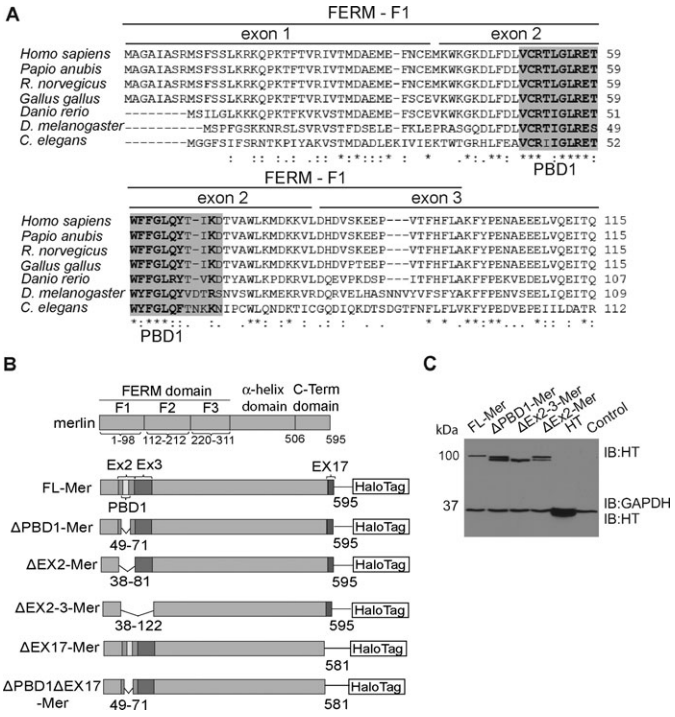

Fig. 1. The conserved PDB1 domain, organization of merlin, and HaloTag® constructs used. (**A**) Comparison of Merlin FERM-domain regions of different species encoded by exons 1, 2, and 3 of *NF2*. Amino acids sequences of *Homo sapiens* (isoform 1, GeneBank Accession No: NP_000259), *Papio anubis* (GeneBank Accession No: AAO23133), *Rattus norvegicus* (GeneBank Accession No: AAR91694), *Gallus gallus* (GeneBank Accession No: NP_989828), *Danio rerio* (GeneBank Accession No: AAS66973), *Drosophila melanogaster* (GeneBank Accession No: AAB08449), and *Caenorhabditis elegans* (GeneBank Accession No: AAA19073) were aligned using ClustalW2. Boundaries among sequences were defined according to the human merlin protein. Gray boxes indicate the PBD1 domain of merlin and bold letters denote identical or conserved amino acids. (*) identical, (:) conserved substitutions, and (.) semi-conserved substitutions. (**B**) Domain organization of merlin and diagrams of merlin Halo®Tag (HT) constructs are shown here. The FERM domain consists of three subdomains, designated F1, F2 and F3. The central region is predicted to have a high α-helical content. Numbers represent amino acid positions in human merlin FL isoform 1 and the position of deletions are indicated by inverted carets (v). (**C**) Western blot showing the expected size of merlin HT constructs (100 kDa) in rat SCs. HT plasmid (control) produced a band at approximately 30 kDa.

AAF23322, respectively) members of the FERM superfamily of proteins, no conserved alignment was observed for PBD1 (data not shown).

PBD1 increases merlin stability in Schwann cells

To test the influence of PBD1 on merlin stability, we cloned different deletion constructs in HaloTag® (HT) vectors (Fig. 1B) and placed the corresponding cDNAs from merlin isoform-1 (AAA36212) under the control of a strong (C14) and 10-fold weaker (C15) cytomegalovirus (CMV) promoter. We confirmed transient expression of merlin HT variants of approximately 100 kDa in SCs by immunoblotting with an HT antibody. Expression of HT alone in SCs yielded a band of approximately 30 kDa (Fig. 1C).

Next, we used a pulse-chase labeling approach to measure the intracellular half-life of full-length merlin (FL-Mer) and deletion variants in SCs. In brief, we transfected cells with HT merlin constructs, pulse labeled with HaloTag® TMR Ligand (TMR), and chased for the indicated times in the presence of a blocking ligand. TMR fluorescence was quantitated from the gel and total HT tagged protein was quantitated from western blots by chemiluminescence. We used the ratio of TMR intensity to HT antibody intensity to assess the rate of degradation by exponential decay regression analysis. Merlin variants ΔPBD1, ΔEx2, and ΔEx2–3, all of which lacked PBD1, exhibited similar degradation rates with half-lives ranging from 3.4 to 4.5 hours. These variants were degraded nearly three times faster than FL-Mer, which had a half-life of 11 hours (Fig. 2A,B). The HT blot indicated that the total amount of expressed protein did not change over the chase period. In addition, the unconjugated HT peptide had a half-life of approximately 17 hours, indicating that the tag was not responsible for the observed rapid degradation.

Merlin and deletion variants are degraded by the ubiquitin-proteasome pathway

We assessed the role of the proteasome in merlin degradation using MG132, a specific proteasome inhibitor (Kisselev and Goldberg, 2001). MG132 added during the pulse-chase period reduced degradation of FL-Mer and the merlin deletion variants as evidenced by a constant level of TMR fluorescence for all constructs (Fig. 2C). Consistent with protein accumulation, the HT blot revealed an increase in the amount of expressed HT tagged protein for all variants in the presence of MG132. Next, we examined merlin ubiquitination in the presence and absence of MG132 for 6 hours. Total protein extracts were immunoprecipitated with an HT antibody and probed with an ubiquitin antibody. The HT blot showed merlin variants at their expected sizes, while the ubiquitin blot exhibited a weak, high

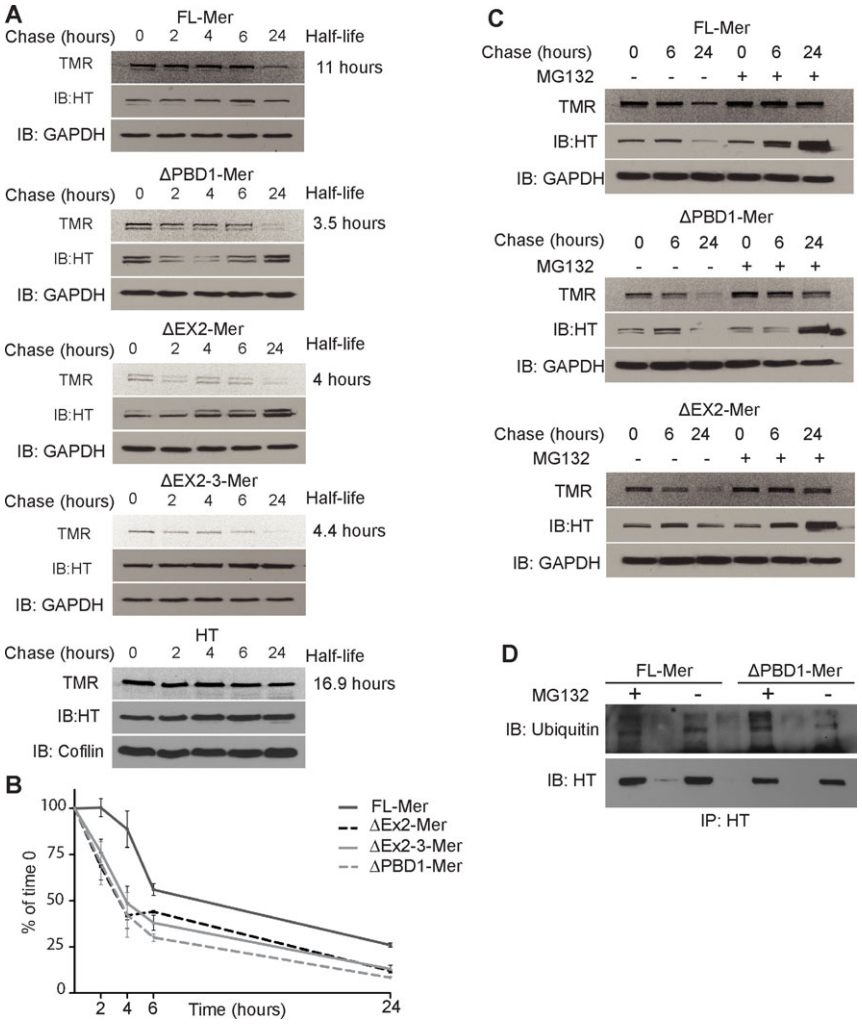

Fig. 2. Merlin variants are unstable in primary rat Schwann cells. (**A**) Transfected rat SCs transiently expressing full-length merlin or variants were pulse labeled with TMR ligand and chased for 0, 2, 4, 6, and 24 hours. Equal amounts of protein extracts were separated by SDS-PAGE and labeled proteins were quantified by fluorescent image analysis (TMR). Immunoblots were conducted with HT and GAPDH antibodies. TMR signals were normalized against HT signals. Half-lives were calculated from an exponential decay equation according to the formula, half-life = Ln (2) K, where K is the rate constant expressed in reciprocal units of the x-axis time units. Data were analyzed using GraphPad from three independent experiments. Merlin variants (ΔPBD1, ΔEx2, and ΔEx2–3) were degraded almost three times as fast as FL. (**B**) Fluorescent normalized intensities (TMR/HT) were plotted relative to the amount present at the respective zero time points against time. (**C**) Transfected cells were pulse labeled by HT TMR ligand and treated with 20 μM MG132 or identical amounts of carrier for 6 and 24 hours. Inhibition of the proteasome with MG132 stabilized degradation of merlin FL and variants. (**D**) Total lysates of transfected cells were immunoprecipitated (IP) and immunoblotted (IB) with the indicated antibodies confirming the ubiquitination of merlin in these experiments.

molecular weight smear in lanes treated with MG132 (Fig. 2D). This shift is typical of polyubiquitinated proteins and these results are consistent with proteasomal degradation of merlin and merlin deletion variants.

PBD1 targets merlin to the plasma membrane where it associates with β1 integrin

We previously reported that merlin is present in a β1 integrin complex at the plasma membrane in SCs (Fernandez-Valle et al., 2002). To assess whether PBD1 is required for merlin to associate with β1 integrin on the cell surface, we clustered surface β1 integrins using an antibody targeting the extracellular (EC) domain of intact SCs that had been transfected with the following plasmids: FL-Mer, ΔPBD1-Mer, ΔEx2–3-Mer, ΔEx17-Mer, double deletion ΔPBD1ΔEx17-Mer, and HT. Transiently transfected SCs in suspension were incubated with either β1 integrin-coated or IgM-coated magnetic beads as a control and bound cells were collected and lysed. HT blots of the β1 integrin fraction indicated that only FL-Mer and ΔEx17-Mer were present. None of the merlin constructs lacking PBD1 were detected in the β1 integrin fraction (Fig. 3). The β1 integrin blot confirmed enrichment of integrins in the bound fraction, while all merlin variants were found in the soluble fraction confirming their expression in SCs. We used GAPDH immunoblotting as a marker for soluble proteins and GAPDH was observed in the soluble fraction. HT alone was found only in the soluble fraction (data not shown).

PBD1 is necessary for association of merlin and cortical actin

Next, we studied the cellular localization and detergent resistance of the merlin variants. When we expressed FL-Mer and ΔEx17-Mer in SCs, TMR fluorescence revealed enrichment at the plasma membrane and in the form of long filamentous protrusions, with a weaker homogenous distribution throughout the rest of the cell. By contrast, ΔPBD1-Mer, ΔEx2–3-Mer, and double deletion ΔPBD1ΔEx17-Mer variants were evenly distributed throughout the SC, excluding the nucleus. Plasma membrane localization was not observed (Fig. 4). After extraction of SCs expressing FL-Mer and ΔEx17-Mer, only the characteristic filamentous distribution remained. This insoluble pool of merlin colocalized with F-actin. Little paxillin fluorescence was observed after detergent extraction, indicating that the majority of paxillin was soluble. Deletion variants lacking PBD1 were completely extracted after detergent treatment and no TMR fluorescence was observed (Fig. 5).

Because overexpression of merlin with the strong C14 promoter may not accurately reflect normal distribution of the endogenous protein, we repeated the experiment using a weaker C15 promoter. FL-Mer expressed using both C14 and C15 promoters resisted detergent extraction, but the characteristic

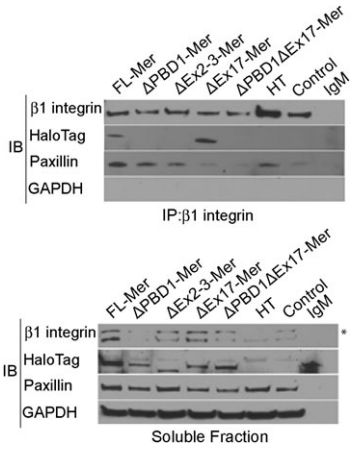

Fig. 3. Merlin lacking PBD1 does not associate with clustered β1 integrins. Rat SCs were transiently transfected with HT-fused merlin FL and variants. Surface β1 integrins were clustered on live SCs with an IgM against β1 integrins covalently linked to magnetic beads. Bound SCs were lysed in CSK buffer and the soluble fraction and β1 integrin-associated insoluble proteins (IP) were analyzed by SDS-PAGE and immunoblotting. None of the variants lacking PBD1 (ΔPBD1, ΔEx2–3, and double deletion ΔPBD1ΔEx17) were found in the IP fraction, while all tested constructs were present in the soluble fraction, as observed in the IB:HT lanes. GAPDH was used as a soluble protein marker. The same number of cells was used for all variants and twice the volume was loaded in the IP lane compared to the soluble fraction lane. (*) denotes a non-specific interaction.

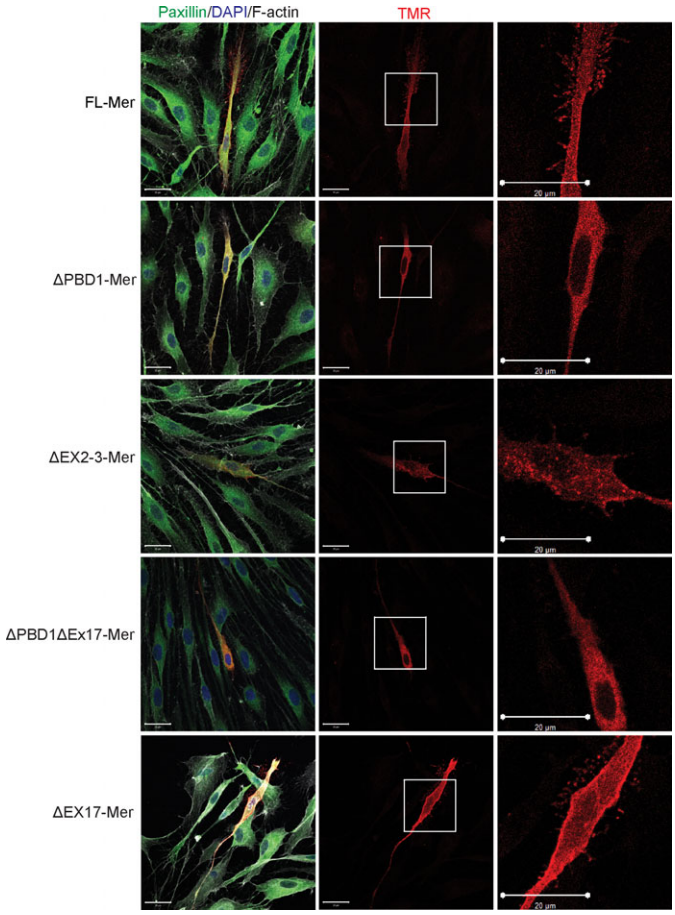

Fig. 4. PBD1 targets merlin to the plasma membrane and promotes formation of membrane protrusions. The subcellular localization of HT-fused FL merlin and other variants is shown in transfected SCs. Fixed cells were labeled with the TMR ligand. Merlin FL and ΔEx17 were found in the cytoplasm and had filamentous membrane structures. ΔPBD1, ΔEx2–3, and double deletion ΔPBD1/ΔEx17 variants localized to the cytoplasmic region and no membrane protrusions were observed. Left panels show merged pictures with positive transfected cells (red). Center panels show TMR-labeled SCs expressing merlin. Right panels show enlargements of the insets in the center panels. Merlin subcellular localization and membrane structures are visualized by TMR labeling (red). Scale bar: 20 μm. DAPI (blue) was used to visualize nuclei, phalloidin (white) to detect F-actin, and paxillin (green) to visualize cell morphology.

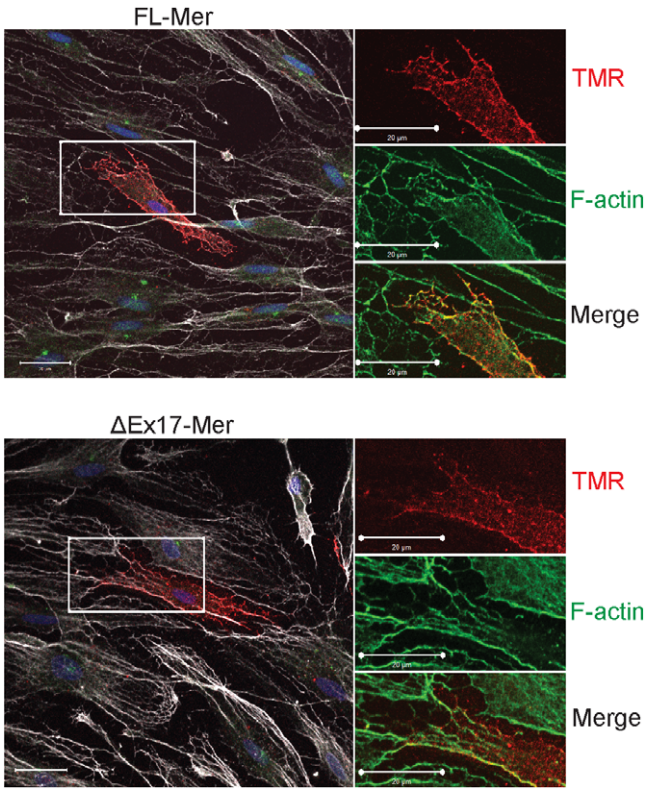

Fig. 5. PBD1 allows association of merlin with F-actin. Cells transfected with HT-fused merlin and variants were labeled with TMR ligand (red), extracted on ice with 0.5% Triton X-100 (TX-100), and fixed. Merlin FL and ΔEx17 were partially resistant to TX-100 extraction and exhibited a filamentous distribution that colocalized with F-actin. No expression of ΔPBD1, ΔEx2–3, and ΔPBD1/ΔEx17 variants was observed after TX-100 extraction. Scale bar: 20 µm. Merlin was visualized by TMR labeling (red). F-actin was stained with phalloidin (white and green in enlargement).

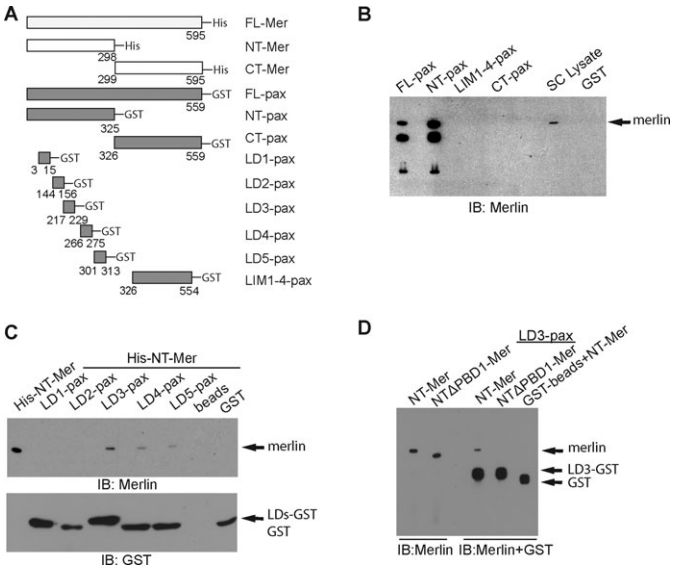

Fig. 6. Paxillin interacts with merlin through its LD3, 4, and 5 domains. Direct binding assays of paxillin-GST and merlin-His fusion proteins are shown here. (**A**) Diagram of merlin and paxillin constructs used. (**B**) GST-paxillin fusion proteins were incubated with SC total cell extract (TE). Positive interactions between merlin and paxillin full-length (FL) and paxillin N-terminus (NT) were observed. (**C**) Paxillin fusion proteins were incubated with merlin-NT. A positive interaction was found for paxillin LDs 3, 4, and 5. GST immunoblots were used as a control. (**D**) Paxillin LD3 fusion proteins were incubated with merlin-NT and NTΔPBD1. No positive interaction was observed in the merlin variant lacking the PBD1 sequence.

filamentous distribution was observed only when the weaker C15 promoter was used. When the stronger promoter was used, a punctate distribution for FL-Mer was observed, suggesting formation of protein aggregates (supplementary material Fig. S2). On the other hand, ΔPBD1-Mer and ΔEx2–3-mer variants were only detected after detergent extraction when expressed under the C14 promoter and both deletion variants exhibited a punctate rather than filamentous distribution (supplementary material Fig. S2). Therefore the higher level of merlin expression could lead to erroneous conclusions that do not reflect the localization of the endogenous merlin.

Paxillin LD3 domain binds merlin PBD1

Finally, we identified paxillin domains which bind directly to merlin. We expressed several merlin (*Homo sapiens*, NP_000259) and paxillin (*Gallus gallus*, NP_990315) constructs *in vitro* (Fig. 6A). Paxillin variants were tagged with glutathione-S-transferase (GST) and merlin variants were tagged with His. Full-length (FL-pax) and N-terminus (NT-pax) paxillin bound endogenous merlin in confluent SC extracts, while C-terminus paxillin (CT-pax) and paxillin LIM domains (LIM1–4-pax) did not (Fig. 6B), suggesting that merlin binds to the N-terminus of paxillin. To identify if the LD domains mediate binding to merlin, we conducted direct binding assays using paxillin LD-GST and merlin His fusion proteins. We found that LDs 3, 4, and 5, but not LDs 1 or 2, interacted with NT-Mer (Fig. 6C). In addition, NT-Mer did not bind the GST-beads or naked beads, indicating that merlin binding to paxillin LDs 3, 4, and 5 was specific. Because LD3 binding to other proteins has not been reported and it has been suggested that LD3 is a pseudo-domain (Brown and Turner, 2004), we tested the specificity of its binding to merlin by incubating merlin deletion variants with LD3-GST. NT-Mer was detected in the LD3 lane, but was not observed when PBD1 was deleted from NT-Mer (NTΔPBD1-Mer). These results demonstrate that the merlin N-terminus binds to paxillin LDs 3, 4, and 5, and PBD1 binds directly to paxillin LD3 (Fig. 6C,D).

Discussion

In this study, we investigated the role of PBD1 in merlin stabilization and the interaction of PBD1 with a β1 integrin complex at the plasma membrane. We demonstrated that the PBD1 domain is necessary and sufficient for merlin stabilization in SCs and that it directly binds to the LD3 domain in the N-terminus of paxillin.

PBD1 is a conserved domain among ERM proteins

Sequence similarity among ERM proteins is found in the FERM domain and phylogeny studies have indicated that ERM proteins and merlin form an orthologous group originating in the earliest metazoans (Bretscher et al., 2002). The PBD1 sequence is similarly conserved as it exhibits a high degree of conservation in metazoans, including worms and insects. Interestingly, PBD1 is the only conserved region in the F1 sub-domain, with 15 of 21 identical or highly conserved amino acids, indicating a high degree of evolutionary constraint and functional conservation.

PBD1 confers merlin stability

Multiple observations confirm the importance of PDB1 in merlin functioning. For example, a high frequency of mutations in exon 2 of *NF2*, which encodes the PDB1 sequence, has been observed in NF2 patients and conditional deletion of this exon ($Nf2^{flox2}$) results in development of schwannomas in animals (Giovannini et al., 2000). Merlin lacking exon 2 is not readily detected in these animals and a merlin isoform with an in-frame deletion of both exons 2 and 3 appears to be rapidly degraded by the ubiquitin-dependent proteasome pathway (Gautreau et al., 2002). Our studies confirmed these observations and demonstrated that variants lacking exons 2 and 3 were degraded three times faster than full-length merlin in a proteasome-dependent manner. Furthermore, building on these observations, we found that merlin's resistance to degradation depends almost entirely on the PBD1 domain encoded by exon 2. We propose that merlin lacking PBD1 is rapidly degraded because it is unable to associate with paxillin and be targeted to the plasma membrane, suggesting that merlin on the plasma membrane may have a different half-life than its cytosolic counterparts. Similar observations have been made for many peripheral membrane proteins, whereby their stability increases with recruitment to the plasma membrane and incorporation into multi-protein complexes. The disparate properties of membrane- and cytosol-associated merlin raise a number of interesting questions and suggest that the tumor suppressor activity of merlin, which has been ascribed to the cytosolic form of the molecule, may be regulated by rapid turnover. Our observations provide new insights into the molecular pathology underpinning NF2 involving mutations in exons 2 and 3.

PBD1 interacts with actin and β1 integrin at the plasma membrane

Merlin, similar to ERM proteins, influences cytoskeleton dynamics, and when merlin is absent in SCs, dramatic alterations in the actin cytoskeleton are observed (Gonzalez-Agosti et al., 1996; Lallemand et al., 2009a). Merlin overexpressed in SCs localizes to the plasma membrane and triggers the development of filamentous protrusions (Fernandez-Valle et al., 2002; Lallemand et al., 2009b). A number of mechanisms and protein interactions have been proposed to regulate the localization of merlin to the plasma membrane, including the formation of heterotypic complexes with other members of the ERM family such as ezrin (Grönholm et al., 1999; Gutmann et al., 1999). We examined this possibility using merlin ΔEx17, a deletion variant that is unable to self-associate or interact with other members of the ERM family. Our results suggest that the paxillin interaction via PBD1 is necessary and sufficient for merlin targeting to the plasma membrane. First, constructs lacking PBD1 localized to the cytosol and had no filamentous structure. Second, merlin colocalized with cortical F-actin at or near the plasma membrane, and although merlin lacks the canonical actin-binding site found in other ERM proteins, sites of indirect association with actin have been defined in other areas of the molecule, particularly in the N-terminus (Deguen et al., 1998; Brault et al., 2001). We observed merlin colocalization with F-actin only when PBD1 was present, suggesting that paxillin binding is important for merlin's indirect interaction with actin. Along these lines, another interesting observation is the conservation of the PBD1 domain among other ERM family members suggesting a conserved ability to associate with paxillin. The importance of this observation is the subject of ongoing investigation in our laboratory.

During myelination dramatic changes in SC morphology take place, many of which depend on the interaction of the SC and the ECM through formation of β1 integrin complexes. We previously reported that merlin is instrumental in the association of these β1 integrin complexes with the actin cytoskeleton (Obremski et al., 1998) and that this association appears to involve paxillin in a density-dependent manner (Fernandez-Valle et al., 2002). Here, we confirmed and extended these observations by demonstrating that merlin lacking PBD1 was not found in β1 integrin clusters formed at the plasma membrane even though a pool of soluble merlin variants was observed for all constructs.

Merlin binds to paxillin LD domains

The paxillin scaffold protein is a key player in β1 integrin signaling pathways because it facilitates assembly of multi-protein signaling complexes localized at focal adhesions (Brown and Turner, 2004). Paxillin LD motifs, encoded in the N-terminal domain, interact with several proteins associated with remodeling of the actin cytoskeleton including FAK, vinculin, and PAK. Different proteins can bind the same LD domain as well as interact with multiple LDs, indicating a level of redundancy between the different LD domains. For example, vinculin binds LD1, 2, and 4; actopaxin binds LD1 and 4; and FAK and Pyk2 bind LD2 and 4 (reviewed by Tumbarello et al., 2002). It has been hypothesized that redundancy in LD interactions could be advantageous for large protein complex formation, although relative affinities of each paxillin binding partner for individual LD motifs could be an important factor in complex assembly (Robertson and Ostergaard, 2011). To date no interactions or binding partners had been attributed to the LD3 domain (Hoellerer et al., 2003; Brown and Turner, 2004). In this study, we used a direct binding assay to demonstrate that the merlin N-terminus binds to paxillin LDs 3, 4, and 5. Moreover, we showed that deletion of PBD1 from the merlin N-terminus abrogates LD3 binding, thus identifying the first known binding partner of the LD3 domain of paxillin.

Based on the crystal structure of the merlin FERM domain alone (Kang et al., 2002), we propose a three-dimensional model of the merlin-PBD1 interaction with paxillin-LD4. Using SWISS-Pdb Viewer (Guex and Peitsch, 1997), we determined that PBD1 lies at the exterior of the merlin three-dimensional structure, and thus, is available for interaction with paxillin LD domains. By superposing this structure with the one reported for LD4 in complex with the focal adhesion kinase (FAK) targeting domain, FAT, a fit is predicted (Fig. 7A). The three point mutations reported in NF2 patients (Trp60Cys, Phe62Ser, and Leu64Pro) which occur within PBD1 are highlighted in the model. There is a predicted molecular interaction between Trp60 and Glu4 in LD4 of paxillin when bound to the FAT domain of FAK. This interaction is lost in the Trp60Cys mutant (Fig. 7B). Additionally, when the crystal structure of the reported merlin closed conformation is used, a fit with the LD4-paxillin is no longer predicted (Yogesha et al., 2011) (PDB ID 3U8Z; data not shown). This provides supporting evidence for a direct interaction between PBD1 in the open merlin conformation and paxillin LD3–5 domains possibly when bound to FAK. This is consistent with our previous report demonstrating that merlin, paxillin and focal adhesion kinase form a complex with β1 integrin at the SC surface (Fig. 7C) (Taylor et al., 2003).

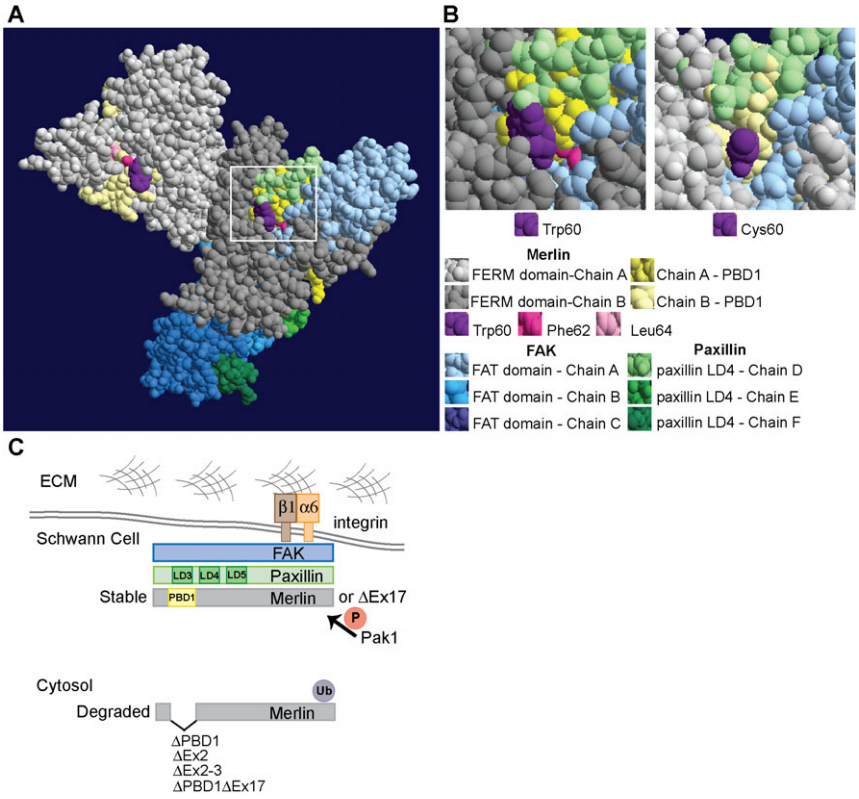

Fig. 7. Model of merlin-paxillin interaction. (**A**) Representation of a potential complex between the FERM domain of merlin and the paxillin LD4 motif based on published crystal structures. The crystal structure of merlin FERM domain (PDB ID: 1H4R) was superposed with paxillin LD4 motif bound to the focal adhesion kinase (FAK) targeting domain (FAT) (PDB ID: 1OW7). PBD1 (amino acids 50–70; yellow) are exposed in the merlin FERM domain allowing potential binding to paxillin LD domains (green). Naturally occurring missense mutations in PBD1, Trp60Cys, Phe62Ser, and Leu64Pro are shown (pink/purple). All structures are shown as molecular surfaces. (**B**) Enlargement of PBD1 Tryp60 region. When the non-polar Trp60 is mutated to the polar Cys the interface architecture is changed and the interaction of residue 60 with Glu4 of LD4 is lost. (**C**) Merlin PBD1 potentially interacts with the paxillin LD3–5 bound to FAK. This interaction targets and/or stabilizes merlin at the plasma membrane and allows association with β1 integrin and actin. These associations protect merlin from degradation by the ubiquitin-proteasome pathway. Merlin lacking PBD1 remains in the cytosolic compartment and is rapidly degraded. ECM: extracellular matrix. PAK: p-21-activated kinase.

In sum, numerous observations suggest an important functional role for amino acid sequences encoded by exon 2 of the merlin gene. In this study, we demonstrated conservation of this sequence, PBD1, in members of the ERM family and showed that it is necessary and sufficient for membrane localization of merlin driven by association with LD domains 3, 4, and 5 of paxillin. In addition, we showed that this interaction is important for the stabilization of merlin and that cytosolic isoforms of the molecule incapable of interacting with paxillin are rapidly degraded in a proteasome-dependent manner. These findings are important for understanding of the molecular pathology of NF2, particularly those cases associated with mutations in exon 2 of the *NF2* gene.

Materials and Methods

Antibodies and western blotting

The following antibodies were used: mouse monoclonal against GAPDH (1:1000, Millipore); rabbit monoclonal against integrin beta-1/CD29 (Epitomics); hamster monoclonal against anti-rat CD29 (BD Pharmagin); monoclonal hamster IgM, λ Isotype control (BD Pharmagin); rabbit polyclonal against HT (1:4000, Promega); mouse monoclonal against Paxillin (1:2000, BD Pharmagin), rabbit polyclonal against merlin (C18 and A19, Santa Cruz Biotechnologies), and rabbit whole serum against ubiquitin (Sigma). Western blotting was carried out using standard protocols. Horseradish peroxidase conjugated secondary antibodies (Jackson Immunoresearch) were used for detection of bound proteins using Super Signal West Pico Chemiluminescent Substrate (Pierce). Signals were measured using the KODAK Image Station 4000MM PRO with selected ROI (regions of interest). Net Intensity was quantified using Carestrem Molecular Imaging Software (Version 5.0).

Cell culture and transfection

Primary rat SCs were obtained from newborn rat sciatic nerves as previously described (Obremski et al., 1998). Cells were plated on uncoated plastic dishes and grown in DMEM with 10% fetal bovine serum (D10). Rapidly dividing fibroblasts were eliminated by growth in D10 containing 10^{-5} M cytosine arabinoside (Sigma-Aldrich, St Louis, MO) for 5 days. SCs were expanded on 200 µg/ml poly-L-lysine (PLL, Sigma-Aldrich, St Louis, MO) coated dishes in D10M [DMEM, 10% fetal bovine serum, 2 µM Forskolin (Sigma-Aldrich, St Louis, MO) and 20 µg/mL Pituitary Gland Extract (Biomedical Technologies, Stoughton, MA). Cultures were passaged no more than 7 times prior to use and checked for purity by assessing cellular morphology. Transfections were carried out using Effectene (Quiagen) according to the manufacturer's instructions. Cultures were used 24–48 h after transfection. For immunostaining experiments, SCs were plated on PLL (200 µg/mL) coated German glass coverslips (Caroline Biol., Burlington, NC). Cells were grown at 37℃, 5% CO_2.

Plasmid construction

Merlin human isoform 1 (NM_000268) and merlin ΔPBD1 (residues 50–70 deleted) in pGEX2TK (Pharmacia) (described in Fernandez-Valle et al., 2002) were used as templates for cloning into HaloTag® (HT) vectors following the manufacturer's instructions (Promega). Fragment amplification was performed using Phusion® High-Fidelity DNA Polymerase (New England BioLabs). The HT plasmid (control, expressing only the Halo Tag) was constructed using primers 5′CGCGTAAGGGTAGGTTT3′ and 5′AAACCTACCCTTACGCGAT3′ by direct annealing and cloned into pFN21A. His-merlin-N terminus (NT, residues 1–298), His-merlin-C terminus (CT, residues 299–595), His-merlin-NTΔPBD1 (residues 50–70 deleted) constructs in pET-28a (+) (Novagen), and GST-paxillin-full length (FL), GST-paxillin-N terminus (NT, residues 1–325), GST-paxillin-C terminus (CT, residues 326–559) constructs in pGEX-6P – 1 vector (Amersham) for prokaryotic expression – were cloned using standard techniques or as previously described (Fernandez-Valle et al., 2002). Paxillin LD1 (residues 3–15), LD2 (residues 144–156), LD3 (residues 216–228), LD4 (residues 265–276), and LD5 (residues 333–345) in pGEX-2TK (Amersham) for prokaryotic expression were a gift from Dr. C Turner (State University of New York at Syracuse). Deletion constructs (ΔEx2, ΔEx2–3) were made using the In-Fusion®EcoDry™ Cloning System from Clontech following manufacturer's instructions. Deletion construct ΔEx17 was made using specific primers. All constructs were confirmed by sequencing.

Pulse-chase analysis

SCs were labeled for 15 min with 50 µM HT TMR Ligand according to the manufacturer's protocol (Promega), at 37℃, 5% CO_2. The HT Ligand is comprised of a linker that covalently binds to the HT protein and a fluorescent moiety (TMR, tetramethylrhodamine). After labeling, cells were washed and incubated in D10M for 30 min to wash away all unbound ligand. Next, cells were incubated with 50 µM HT Succinimidyl Ester (O4) Ligand in D10M as a blocking agent for the indicated chase times and extracted in SDS extraction buffer (Fermentas). Samples were heated at 95℃ for 5 min and equal amounts of samples were loaded and resolved by 10% SDS-PAGE. TMR fluorescence was detected

from the gel with MWL Ex55 Em600 with KODAK Image Station 4000MM PRO and ROI (region of interest) Net Intensity was quantified using Carestrem Molecular Imaging Software (Version 5.0). Western blotting was conducted using standard protocols. Three independent experiments were performed and the half-life was calculated using GraphPad Prism version 5.00 with an exponential decay model (one phase decay, fitting method least square), where half-life is computed as ln (2)/K and K is the rate constant expressed in reciprocal of the x-axis. For the proteasome inhibitor experiment, MG132 ($C_{26}H_{41}N_3O_5$, Calbiochem) was used at a concentration of 20 μM for the indicated times.

Immunoprecipitation

SCs were extracted using TAN buffer (10 mM Tris-acetate pH 8.0, 100 mM NaCl, and 1% IGEPAL) supplemented with protease inhibitors. Equal amounts of lysates were immunoprecipated with 5 μg of HT antibody adsorbed to Dynabeads® Protein G (Invitrogen) overnight at 4℃.

β1 integrin aggregation on SCs

β1 integrin aggregation was performed as previously described (Taylor et al., 2003). Briefly, anti-β1 integrin IgM antibodies (BD) and normal Hamster IgM were coupled with Dynabeads® M-450 Tosylactivated (Invitrogen) according to the manufacturer's protocol. Transfected SCs in suspension were incubated with 10 coated-beads per cell for 30 min at 4℃. Antibody-bound SCs were lysed in CSK lysis buffer (10 mM PIPES, pH 6.8; 50 mM NaCl; 300 mM sucrose, 2 mM $MgCl_2$; 0.5% (v/v) Triton X-100 (TX-100)) with Halt™ Protease Inhibitor Cocktail (Pierce) that enriches for focal adhesion proteins (Plopper et al., 1993). Magnetic beads containing the β1 integrin-associated complex were washed and resuspended in SDS sample buffer (Fermentas).

Immunostaining

Primary rat SC cultures were fixed in 4% paraformaldehyde and permeabilized for 10 min in 0.2% TX-100 before immunostaining. Non-specific binding sites were blocked for 30 min in phosphate buffer containing 10% goat serum (blocking buffer) and primary antibodies diluted in blocking buffer were added to the coverslips for 1 h. Bound antibodies were detected by incubation with secondary antibodies conjugated with fluorescent Alexa Fluor® (Invitrogen) for 30–45 min at room temperature. SCs were post-fixed with 4% paraformaldehyde for 5 min and stained with Alexa Fluor® 633 phalloidin or DAPI (Invitrogen) when indicated and mounted in Gel Mount (ECM Bioscience, CA, USA). To visualize merlin colocalization with F-actin, SCs were extracted on ice for 45 min in CSK extraction buffer (10 mM PIPES, pH 6.8; 50 mM NaCl; 300 mM sucrose, 2 mM $MgCl_2$; 0.5% (v/v) TX-100), and then fixed and permeabilized as already described. All cultures were analyzed with a Zeiss LSM710 microscope and Zen 2009 software. Image acquisition was optimized for each antibody and fluorescence was collected on separate channels using identical parameters for all variants.

In vitro affinity precipitation assay

Expression of recombinant GST fusion proteins was induced in *E. coli* BL21 with 1 mM isopropyl-β-D-1-thiogalactopyranoside (IPTG). Proteins were extracted in a GST lysis buffer (10 mM Tris-HCl, pH 8.0, 100 μl PIC, 1% TX-100) with lysozyme (1 mg/30 mL pellet). Complete bacterial lysis was obtained either by a French press or by sonication, and proteins were purified using glutathione-Sepharose 4B beads (Amersham) according to the manufacturer's recommendations. SCs were extracted using TAN buffer containing protease and phosphatase inhibitors (20 μg/mL aprotinin, 10 μg/mL luepeptin, 1 mM SOV, 1 mM sodium pyrophosphate, 50 mM NaF, 2 mM PMSF). Immobilized GST fusion proteins were incubated overnight at 4℃ with 200 μg of lysate and washed with GST Bind/Wash Buffer containing 0.1% TX-100 before immunoblot analysis.

Direct binding assays

Expression of N-terminal His-tagged merlin proteins was induced in BL21 (DE3) cells with 1 mM IPTG for 4 h at 33℃, and cells were purified using the QIAGEN Ni-NTA kit (QUIAGEN) according to the manufacturer's instructions. GST-paxillin proteins were purified as already described. Immobilized GST fusion proteins were mixed with 0.2 μg of the His-tagged deletion variant or truncated merlin protein in 1 mL of 1× PBS containing 0.1% TX-100 and 500 mM NaCl and incubated overnight at 4℃. Binding was assessed by immunoblotting against merlin with the indicated antibodies.

BLAST search and alignment

Protein sequences were identified from the National Center for Biotechnology Information (NCBI) database (http://www.ncbi.nlm.nih.gov/BLAST) using the BLAST algorithm (Altschul et al., 1997). The CLUSTALW2 program from EBI (Larkin et al., 2007; Goujon et al., 2010) was used for sequence alignment.

Three-dimensional model

The SWISS-MODEL and Swiss-Pdb Viewer 4.0.4 (Guex and Peitsch, 1997) (http://spdbv.vital-it.ch) were used to construct a theoretical model of the interaction between merlin FERM domain (PDB ID: 1H4R) and paxillin LD4 bound to FAT domain (PDB ID: 10W7). Superposing structures were done using Deep View Magic Fit, PAM 20 matrix.

Acknowledgements

This work was supported by NIH grant R01 DC010189-01 to CFV. We thank Andrew Knott for editing the manuscript and Tiffany Fabianac for figure preparation.

Competing Interests

The authors have no competing interests to declare.

References

Ahronowitz, I., Xin, W., Kiely, R., Sims, K., MacCollin, M. and Nunes, F. P. (2007). Mutational spectrum of the NF2 gene: a meta-analysis of 12 years of research and diagnostic laboratory findings. *Hum. Mutat.* **28**, 1-12.

Alfthan, K., Heiska, L., Grönholm, M., Renkema, G. H. and Carpén, O. (2004). Cyclic AMP-dependent protein kinase phosphorylates merlin at serine 518 independently of p21-activated kinase and promotes merlin-ezrin heterodimerization. *J. Biol. Chem.* **279**, 18559-18566.

Altschul, S. F., Madden, T. L., Schäffer, A. A., Zhang, J., Zhang, Z., Miller, W. and Lipman, D. J. (1997). Gapped BLAST and PSI-BLAST: a new generation of protein database search programs. *Nucleic Acids Res.* **25**, 3389-3402.

Brault, E., Gautreau, A., Lamarine, M., Callebaut, I., Thomas, G. and Goutebroze, L. (2001). Normal membrane localization and actin association of the NF2 tumor suppressor protein are dependent on folding of its N-terminal domain. *J. Cell Sci.* **114**, 1901-1912.

Bretscher, A., Edwards, K. and Fehon, R. G. (2002). ERM proteins and merlin: integrators at the cell cortex. *Nat. Rev. Mol. Cell Biol.* **3**, 586-599.

Brown, M. C. and Turner, C. E. (2004). Paxillin: adapting to change. *Physiol. Rev.* **84**, 1315-1339.

Brown, M. C., Curtis, M. S. and Turner, C. E. (1998). Paxillin LD motifs may define a new family of protein recognition domains. *Nat. Struct. Biol.* **5**, 677-678.

Chernousov, M. A., Yu, W. M., Chen, Z. L., Carey, D. J. and Strickland, S. (2008). Regulation of Schwann cell function by the extracellular matrix. *Glia* **56**, 1498-1507.

Deguen, B., Mérel, P., Goutebroze, L., Giovannini, M., Reggio, H., Arpin, M. and Thomas, G. (1998). Impaired interaction of naturally occurring mutant NF2 protein with actin-based cytoskeleton and membrane. *Hum. Mol. Genet.* **7**, 217-226.

Fernandez-Valle, C., Tang, Y., Ricard, J., Rodenas-Ruano, A., Taylor, A., Hackler, E., Biggerstaff, J. and Iacovelli, J. (2002). Paxillin binds schwannomin and regulates its density-dependent localization and effect on cell morphology. *Nat. Genet.* **31**, 354-362.

Gautreau, A., Manent, J., Fievet, B., Louvard, D., Giovannini, M. and Arpin, M. (2002). Mutant products of the NF2 tumor suppressor gene are degraded by the ubiquitin-proteasome pathway. *J. Biol. Chem.* **277**, 31279-31282.

Giovannini, M., Robanus-Maandag, E., van der Valk, M., Niwa-Kawakita, M., Abramowski, V., Goutebroze, L., Woodruff, J. M., Berns, A. and Thomas, G. (2000). Conditional biallelic Nf2 mutation in the mouse promotes manifestations of human neurofibromatosis type 2. *Genes Dev.* **14**, 1617-1630.

Gonzalez-Agosti, C., Xu, L., Pinney, D., Beauchamp, R., Hobbs, W., Gusella, J. and Ramesh, V. (1996). The merlin tumor suppressor localizes preferentially in membrane ruffles. *Oncogene* **13**, 1239-1247.

Goujon, M., McWilliam, H., Li, W., Valentin, F., Squizzato, S., Paern, J. and Lopez, R. (2010). A new bioinformatics analysis tools framework at EMBL-EBI. *Nucleic Acids Res.* **38**, **Suppl 2** W695-W699.

Grönholm, M., Sainio, M., Zhao, F., Heiska, L., Vaheri, A. and Carpén, O. (1999). Homotypic and heterotypic interaction of the neurofibromatosis 2 tumor suppressor protein merlin and the ERM protein ezrin. *J. Cell Sci.* **112**, 895-904.

Guex, N. and Peitsch, M. C. (1997). SWISS-MODEL and the Swiss-PdbViewer: an environment for comparative protein modeling. *Electrophoresis* **18**, 2714-2723.

Gutmann, D. H., Haipek, C. A. and Hoang Lu, K. (1999). Neurofibromatosis 2 tumor suppressor protein, merlin, forms two functionally important intramolecular associations. *J. Neurosci. Res.* **58**, 706-716.

Hoellerer, M. K., Noble, M. E., Labesse, G., Campbell, I. D., Werner, J. M. and Arold, S. T. (2003). Molecular recognition of paxillin LD motifs by the focal adhesion targeting domain. *Structure* **11**, 1207-1217.

Kang, B. S., Cooper, D. R., Devedjiev, Y., Derewenda, U. and Derewenda, Z. S. (2002). The structure of the FERM domain of merlin, the neurofibromatosis type 2 gene product. *Acta Crystallogr. D Biol. Crystallogr.* **58**, 381-391.

Kisselev, A. F. and Goldberg, A. L. (2001). Proteasome inhibitors: from research tools to drug candidates. *Chem. Biol.* **8**, 739-758.

Kissil, J. L., Johnson, K. C., Eckman, M. S. and Jacks, T. (2002). Merlin phosphorylation by p21-activated kinase 2 and effects of phosphorylation on merlin localization. *J. Biol. Chem.* **277**, 10394-10399.

Lallemand, D., Manent, J., Couvelard, A., Watilliaux, A., Siena, M., Chareyre, F., Lampin, A., Niwa-Kawakita, M., Kalamarides, M. and Giovannini, M. (2009a). Merlin regulates transmembrane receptor accumulation and signaling at the plasma

membrane in primary mouse Schwann cells and in human schwannomas. *Oncogene* **28**, 854-865.

Lallemand, D., Saint-Amaux, A. L. and Giovannini, M. (2009b). Tumor-suppression functions of merlin are independent of its role as an organizer of the actin cytoskeleton in Schwann cells. *J. Cell Sci.* **122**, 4141-4149.

Larkin, M. A., Blackshields, G., Brown, N. P., Chenna, R., McGettigan, P. A., McWilliam, H., Valentin, F., Wallace, I. M., Wilm, A., Lopez, R. et al. (2007). Clustal W and Clustal X version 2.0. *Bioinformatics* **23**, 2947-2948.

Li, W., You, L., Cooper, J., Schiavon, G., Pepe-Caprio, A., Zhou, L., Ishii, R., Giovannini, M., Hanemann, C. O., Long, S. B. et al. (2010). Merlin/NF2 suppresses tumorigenesis by inhibiting the E3 ubiquitin ligase CRL4(DCAF1) in the nucleus. *Cell* **140**, 477-490.

Maitra, S., Kulikauskas, R. M., Gavilan, H. and Fehon, R. G. (2006). The tumor suppressors Merlin and Expanded function cooperatively to modulate receptor endocytosis and signaling. *Curr. Biol.* **16**, 702-709.

Morrison, H., Sherman, L. S., Legg, J., Banine, F., Isacke, C., Haipek, C. A., Gutmann, D. H., Ponta, H. and Herrlich, P. (2001). The NF2 tumor suppressor gene product, merlin, mediates contact inhibition of growth through interactions with CD44. *Genes Dev.* **15**, 968-980.

Obremski, V. J., Hall, A. M. and Fernandez-Valle, C. (1998). Merlin, the neurofibromatosis type 2 gene product, and beta1 integrin associate in isolated and differentiating Schwann cells. *J. Neurobiol.* **37**, 487-501.

Plopper, G. and Ingber, D. E. (1993). Rapid induction and isolation of focal adhesion complexes. *Biochem. Biophys. Res. Commun.* **193**, 571-578.

Robertson, L. K. and Ostergaard, H. L. (2011). Paxillin associates with the microtubule cytoskeleton and the immunological synapse of CTL through its leucine-aspartic acid domains and contributes to microtubule organizing center reorientation. *J. Immunol.* **187**, 5824-5833.

Rouleau, G. A., Merel, P., Lutchman, M., Sanson, M., Zucman, J., Marineau, C., Hoang-Xuan, K., Demczuk, S., Desmaze, C., Plougastel, B. et al. (1993). Alteration in a new gene encoding a putative membrane-organizing protein causes neuro-fibromatosis type 2. *Nature* **363**, 515-521.

Schaller, M. D. (2001). Paxillin: a focal adhesion-associated adaptor protein. *Oncogene* **20**, 6459-6472.

Scoles, D. R., Huynh, D. P., Morcos, P. A., Coulsell, E. R., Robinson, N. G., Tamanoi, F. and Pulst, S. M. (1998). Neurofibromatosis 2 tumour suppressor schwannomin interacts with betaII-spectrin. *Nat. Genet.* **18**, 354-359.

Taylor, A. R., Geden, S. E. and Fernandez-Valle, C. (2003). Formation of a beta1 integrin signaling complex in Schwann cells is independent of rho. *Glia* **41**, 94-104.

Thaxton, C., Lopera, J., Bott, M. and Fernandez-Valle, C. (2008). Neuregulin and laminin stimulate phosphorylation of the NF2 tumor suppressor in Schwann cells by distinct protein kinase A and p21-activated kinase-dependent pathways. *Oncogene* **27**, 2705-2715.

Trofatter, J. A., MacCollin, M. M., Rutter, J. L., Murrell, J. R., Duyao, M. P., Parry, D. M., Eldridge, R., Kley, N., Menon, A. G., Pulaski, K. et al. (1993). A novel moesin-, ezrin-, radixin-like gene is a candidate for the neurofibromatosis 2 tumor suppressor. *Cell* **72**, 791-800.

Tumbarello, D. A., Brown, M. C. and Turner, C. E. (2002). The paxillin LD motifs. *FEBS Lett.* **513**, 114-118.

Turner, C. E. (2000). Paxillin interactions. *J. Cell Sci.* **113**, 4139-4140.

Turner, C. E., Glenney, J. R., Jr and Burridge, K. (1990). Paxillin: a new vinculin-binding protein present in focal adhesions. *J. Cell Biol.* **111**, 1059-1068.

Turner, C. E., Brown, M. C., Perrotta, J. A., Riedy, M. C., Nikolopoulos, S. N., McDonald, A. R., Bagrodia, S., Thomas, S. and Leventhal, P. S. (1999). Paxillin LD4 motif binds PAK and PIX through a novel 95-kD ankyrin repeat, ARF-GAP protein: A role in cytoskeletal remodeling. *J. Cell Biol.* **145**, 851-863.

Xiao, G. H., Beeser, A., Chernoff, J. and Testa, J. R. (2002). p21-activated kinase links Rac/Cdc42 signaling to merlin. *J. Biol. Chem.* **277**, 883-886.

Yogesha, S. D., Sharff, A. J., Giovannini, M., Bricogne, G. and Izard, T. (2011). Unfurling of the band 4.1, ezrin, radixin, moesin (FERM) domain of the merlin tumor suppressor. *Protein Sci.* **20**, 2113-2120.